



Serbian Tribology  
Society

# SERBIATRIB '19

16<sup>th</sup> International Conference on  
Tribology



Faculty of Engineering  
University of Kragujevac

Kragujevac, Serbia, 15 – 17 May 2019

## SUBSURFACE MATERIAL CHARACTERISATION BY SIMULATION ON CARBURIZED ROLLING CYCLE FATIGUE TEST SPECIMENS

Szabolcs Szávai<sup>1</sup>, Zoltan Bezi<sup>2</sup>, Levente Béres<sup>3</sup>, Sándor Kovács<sup>4</sup>

<sup>1</sup> Institute of Machine and Product Design, University of Miskolc, Miskolc, Hungary

<sup>2</sup> Bay Zoltán Nonprofit Ltd. for Applied Research, Miskolc, Hungary

<sup>3</sup> Bay Zoltán Nonprofit Ltd. for Applied Research, Miskolc, Hungary

<sup>4</sup> Institute of Physical Metallurgy, Metalforming and Nanotechnology, University of Miskolc, Miskolc, Hungary

\*Corresponding author: szabolcs.szavai@bayzoltan.hu

**Abstract:** *The aim of the research is to determine the metallographical and mechanical properties (residual stresses, hardness, phases and texture) of carburized surfaces using finite element method and study the failure of surface during relative motion, and the possibilities of the test methods, which can give us information about the behaviour of these surfaces. This work focuses on contact fatigue tests and properties.*

*Nowadays it can be established that application of finite element method is a reliable way to simulate carburization. It is possible to determine exact approximation for the hardness and carbon content values near the surface after carburization and quenching, but take into account that the simulation of tempering is still an issue, if the material contains retained austenite, the hardness values of the test will be higher near the surface, because of the retained austenite-bainite transformation, so the simulations had to be validated by carburized cylindrical (disc-like) specimens, made of low alloy case hardening steel (16MnCr5). These specimens were tested with glow discharge optical emission spectroscopy, to measure the chemical composition of the surface layer. It is important to know what kind of residual stresses can be observed in the surface after carburization, therefore it was extensively studied during the simulation. Furthermore the values of the hardness in the surface of the specimens have been determined. Having compared the simulation and experiments, good agreement has been found between the results, so the finite element method was validated successfully.*

*For high cycle rolling fatigue test rollers were manufactured. Two disc fatigue tests were carried out on five rollers. Four tests were stopped due to trigger sign by surface damage, while one of those was stopped due to break of the shaft after one millions of rotation. Microstructural investigations have been started on the rollers.*

**Keywords:** *Fatigue, rolling contact, surface treatment, failure, FE analysis*

### 1. INTRODUCTION

The typical damage to the life of the contact surface pairs, such as bearings or gears, is fatigue. From the point of view of failure, the most critical zones appear at the edges of the

contact area or are formed shortly below the surface. Surfaces are subject to high-cycle fatigue, however, the global damage accumulation methods are not applicable.

Although the answer to questions about the lifetime and condition of the parts is

crucial, and while numerical and experimental methods are highly evolving, and modern testing methods are becoming more and more capable of characterizing such tribological events, there are still problems that require further multidisciplinary research.

Local strain energy density models based on kinematic or isotropic hardening material laws are the most promising for local determination of damage. In addition, mechanical properties of the surface should be known for its solution, however the determination or prediction of these properties are also challenging because of the surface treatments.

As a basis for the experimental work, due to the frequent application and previous experience, the 16MnCr5 case hardening steel was selected. On the disc samples made from model material, after the treatment, the tests were carried out to validate the numerical model suitable for determining the characteristics of the near-surface layer properties. By comparing the results, the model has been proved to be suitable for determining the layer characteristics of the rollers used for contact fatigue testing.

## 2. VALIDATION EXPERIMENTS

It is possible to determine exact approximation for the hardness and carbon content values near the surface after carburization and quenching, but take into account that the simulation of tempering is still an issue, so if the material contains retained austenite, the hardness values of the test will be higher near the surface, because of the retained austenite-bainite transformation, so the simulations had to be validated by carburized cylindrical (disc-like) specimens, made of low alloy case hardening steel (16MnCr5). The average chemical composition is shown in the Table 1.

**Table 1.** Chemical composition

C %	Si %	Mn %	P %	S %	Cr %
0.14 - 0.19	0.4	1.0 - 1.3	0.025	0.035	0.8 - 1.1

Carburization, quenching and tempering of 50 mm diameter, 10 mm wide disc-like 16MnCr5 grade specimens were performed. The carbonizing agent was BaCO<sub>3</sub> charcoal activator, 10%, after carbonizing, the specimens were quenched in oil and stress relief annealing was performed (Fig. 1).

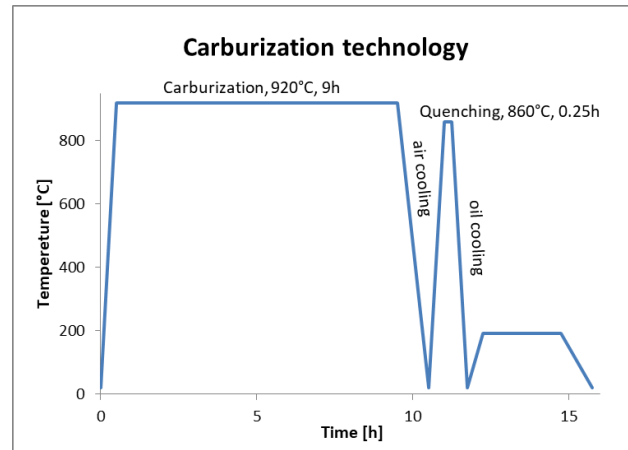


**Figure 1.** Heat treatment temperature-time diagram

The specimens were polished after cutting, and the surface of the specimen was etched with HNO<sub>3</sub> (nitric acid) 2% solution (nitrate etching agent) to show the carbonized layer. The cross section after preparation is shown in Fig. 2.



**Figure 2.** Specimen before hardness measurement

The hardness measurement of the specimen was carried out from outside to inside. The test was done by 0.05 and 0.1 mm increments. The thickness of the hard layer was also determined by measuring the hardness of the core before starting the measurement series, which in this case was 389 HV0.1. The boundary of the carbonized layer was marked with a hardness of 500 HV0.1 corresponding to the hardness of the hardened steel. Due to the determination of this layer thickness, 0.05 mm increments were taken near the boundary of the hardness. Based on the measurement results, a 1.65 mm carbonized layer was reached on the specimen using the applied technological parameters. Figure 3 illustrates a series of measurements with a microscope-mounted

camera showing impressions and the average of the measurement results and distance from the surface at a given point. The distances are in millimeters and the hardness values are in HV0.1

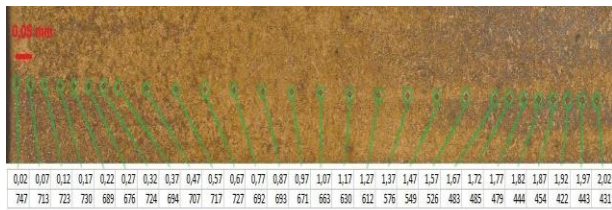


**Figure 3.** Indentation on the surface

These specimens were tested with glow discharge optical emission spectroscopy, to measure the chemical composition of the surface layer. The result of the test shows that after the cementation a layer of carbon content of about 1.4% was formed on the surface. As a result of the test technique, the chemical composition of the surface was analyzed only up to 60  $\mu\text{m}$ , the result of which confirms that when the carburisation is applied near the surface, the carbon content is significantly increased, then the measurement is continued in the direction of the core, the carbon content decreases as expected (Figure 6a).

In solid-cement carburisation, the maximum carbon content cannot be well controlled: the carbon content of charcoal is very high, so that the surface layer is also formed. The 1.4% carbon content determined by the measurement is too high because the amount of residual austenite is significant, which impairs the surface properties. This surface layer can be removed if necessary after finishing machining the parts (finishing, grinding).

### 3. NUMERICAL MODELL DEVELOPMENT

In order to validate the accuracy and dependability of FE simulation, experimental results of carburization of a cylindrical specimen are used to compare with the simulation results of FEM. During the process of the heat treatment cycle coupled thermo-metallurgical and mechanical calculations were carried out by considering the effect of carbon content and incorporating multi-phase transformation models. Numerical calculations

were performed with commercial finite element software package Simufact.forming. The problem was solved numerically in a cylindrical coordinate system due to axial symmetry of the geometry. The geometry and finite element representation used in the modelling is shown in Fig. 4.

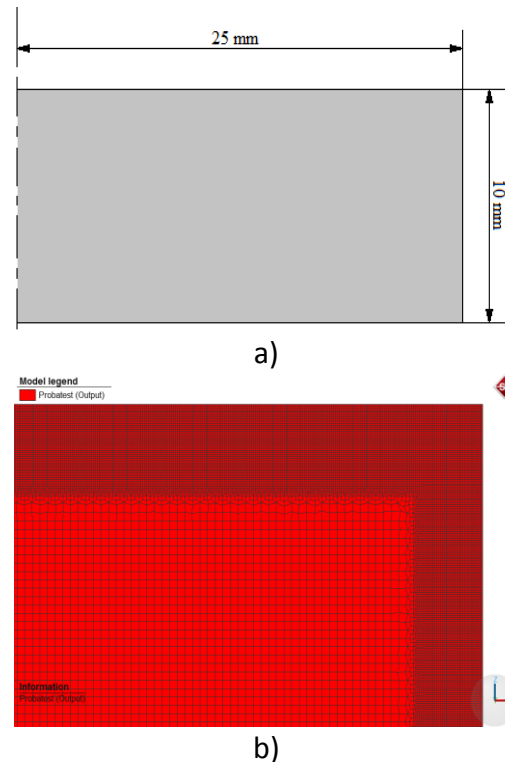


**Figure 4.** Geometry used in modeling

Four-node axisymmetric elements were used to model the specimens. Solid elements were employed to simulate the thermo-elastic-plastic behaviour of the specimen. The mesh is graded from fine to coarse according to the expected reduction in carbon content on moving away from the outer surface.

The mesh contained two-dimensional rectangular elements in the carburised layer 0.05 in the core layer 0.2 mm.

The temperature-dependent mechanical and thermal properties were taken into account in the calculations. The equilibrium transformation temperatures for the formation of austenite from an initial microstructure and the decomposition of austenite into ferrite and martensite are required in the heat treatment simulations. Material properties, based on their chemical composition, were determined using JMatPro software. The temperature-dependent, elastic-

plastic isotropic hardening phase-dependent material model was used in the calculation. The thermo-metallurgy material properties of 16MnCr5 steel were generated with JMatPro software using the average chemical composition which can be seen in Table 1. Transformation data was calculated using Simufact.premap interface with 30 μm grain size starting at 920°C temperature.

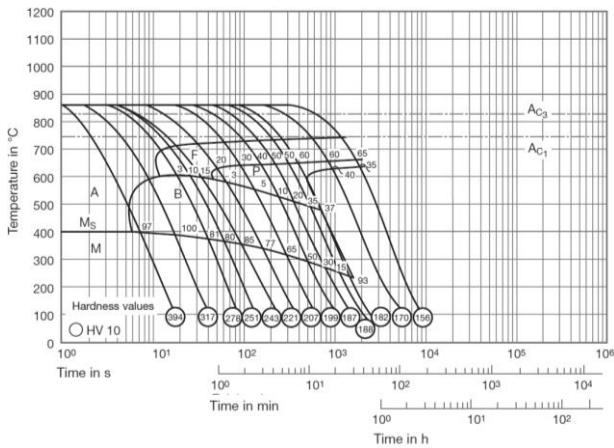


**Figure 5.** Continuous time-temperature-transformation diagram for 16MnCr5 [1]

The equilibrium transformation start temperatures for different carbon content were determined from the literature.

The numerical solution for the carburizing process can be expressed based on mass diffusion. Carbon atoms transfer from the atmosphere to the steel surface during carburizing and diffuse into the steel, which creates a carbon concentration gradient. The governing equations for diffusion-controlled carburizing are:

$$\frac{\partial C\%}{\partial t} = D \frac{\partial^2 C\%}{\partial x^2} \quad (1)$$

where C is the carbon concentration, D is the diffusivity of carbon in austenite, t is time, and x is the average carbon atom diffusion distance. In the simulation, the carbon diffusivity was determined according to the Tibbetts [2] proposed relationship:

$$D(T, C\%) = 0.47e^{-1.6C\%} e^{-\frac{154893-27629C\%}{RT}}, \quad (2)$$

where D is the diffusivity of carbon in cm<sup>2</sup>/s, C% is the carbon content in mass percent, R is the gas constant in 8.314 J/mol/K, and T is the temperature in Kelvin.

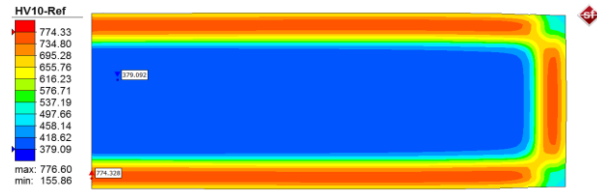
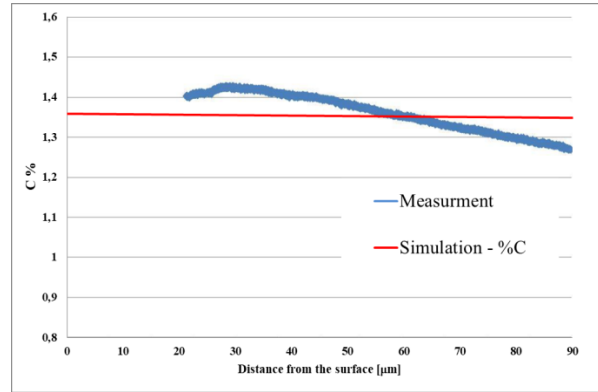
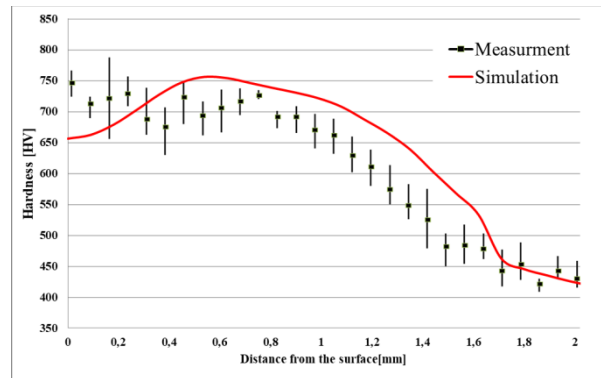


**Figure 6.** The calculated hardness distribution in the specimen



a) Measured and calculated carbon content



b) Measured and calculated hardness

**Figure 7.** Comparison of measured and calculated results

Maynier and coworkers [3] have developed a useful method to predict steel hardness. The total hardness of steel is calculated dependent on the volume fractions of the constituents of the microstructure:

$$HV = (FP\% * HV_{F-P} + B\% * HV_B + M\% * HV_M)/100, \quad (3)$$

The hardness of the microstructures produced are given by:

$$HV_M = 127 + 949C\% + 27Si\% + 11Mn\% + 16Cr\% + 8Ni\% + 21\log v_R, \quad (4)$$

$$HV_B = -323 + 185C\% + 330Si\% + 153Mn\% + 144Cr\% + 191Mo\% + 65Ni\% + (\log v_R)(89 + 53C\% - 55Si\% - 22Mn\% - 20Cr\% - 33Mo\% - 10Ni\%), \quad (5)$$



$$HV_{F-P} = 42 + 223C\% + 53S\%i + 30Mn\% + 7Cr\% + 19Mo\% + 12.6N\%i + (\log v_R)(10 - 19Si\% + 8Cr\% + 4Ni\% + 130V\%) \quad (6)$$

where:  $v_R$  is the cooling rate in K/h.

The hardness values were calculated using the correlations published by Maynier [3] et al at 0.5 C%, while Leslie [4] suggested the relationship with higher carbon content:

$$HV = 1667C\% - 926C\%^2 + 150. \quad (7)$$

The results obtained are illustrated in Fig. 6.

#### 4. FATIGUE TEST ROLLERS

As it was presented above the simulation were good agreement with the experiments, so the model has been proved to be suitable for determining the layer characteristics of the rollers used for contact fatigue testing.

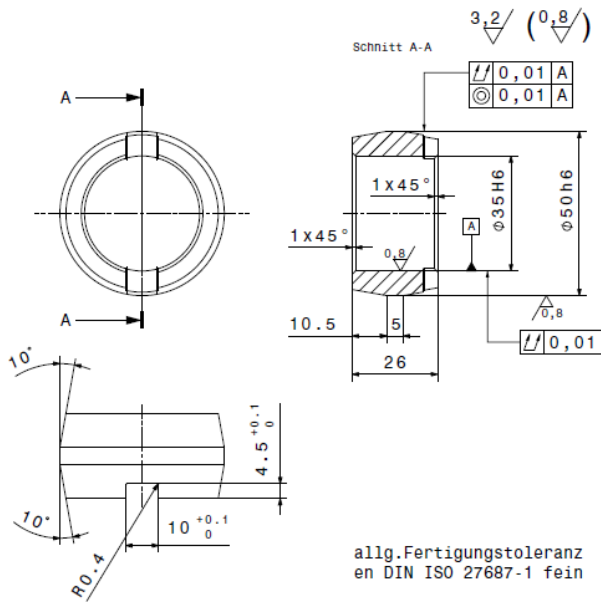


Figure 8. Test rollers' geometry

The geometry of the rollers (Figure 8) was defined by Montanuniversität Leoben, Lehrstuhl für Allgemeinen Maschinenbau (AMB) since as part of our bilateral cooperation the two disk high cycle contact fatigue tests were performed by AMB.

Rollers surface were treated with the described technology. In order to study the near surface properties, the sub-surface stresses, phases and the hardness have been calculated with the verified methodology.

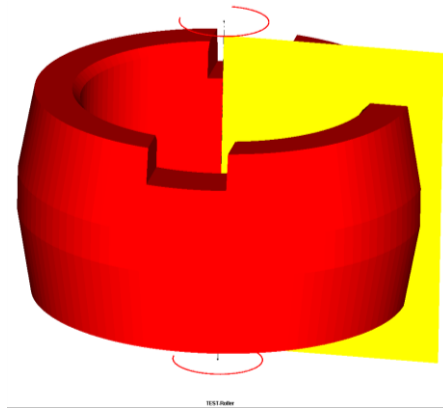


Figure 9. FEM model of the roller

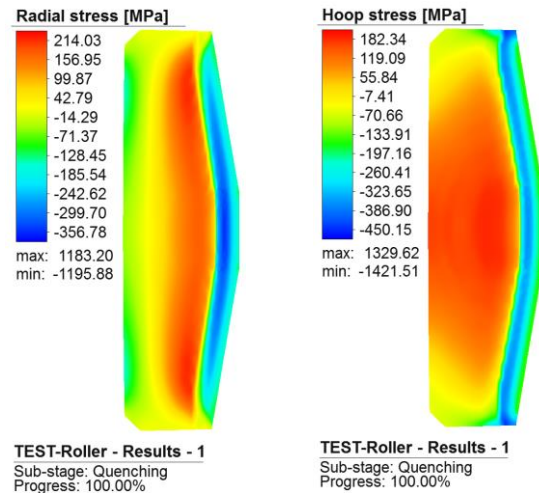


Figure 10. Subsurface stresses

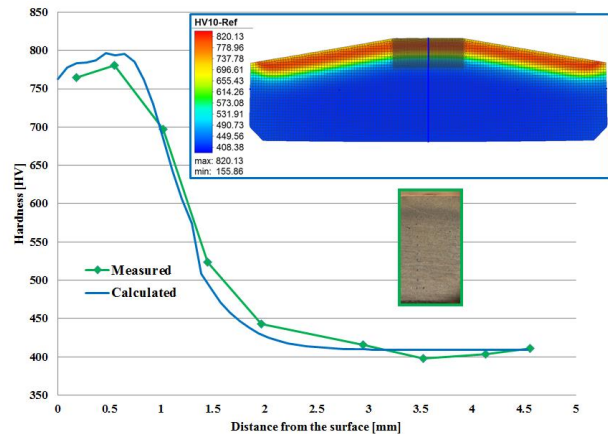


Figure 11. Hardness HV10

#### 5. FATIGUE TESTS

Two disc fatigue tests were carried out on five rollers with different contact force. Four tests were stopped due to trigger sign by surface damage, while one of those was stopped due to break of the shaft after one millions of rotation.

**Table 2.** Cycles to failure

disk	p [GPa]	N [Cycles]	comment
TP1	2.25	4519100	TP2: shaft failure due to fretting
TP2	2.5	1024160	
TP3	2.75	1689382	
TP4	2.22	8028606	
TP5	2.5	7857350	

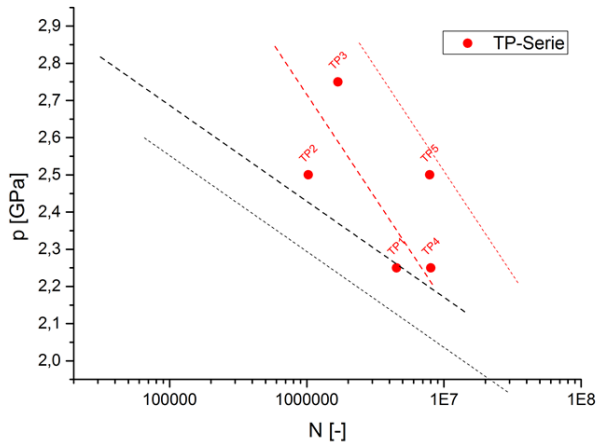


**Figure 12.** Test results

After the tests the rollers have been cut to pieces and microstructural investigations have been started on the rollers. Pieces of TP2 specimen can be seen on Fig. 13.



**Figure 13.** Pieces of TP2 specimen

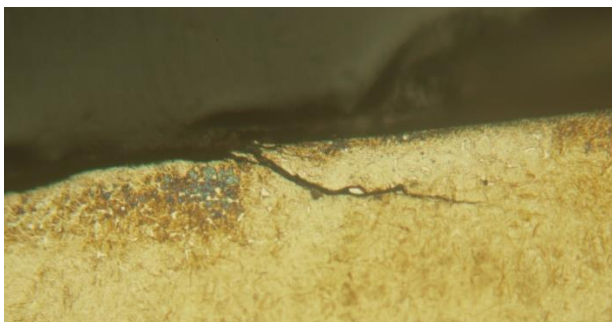
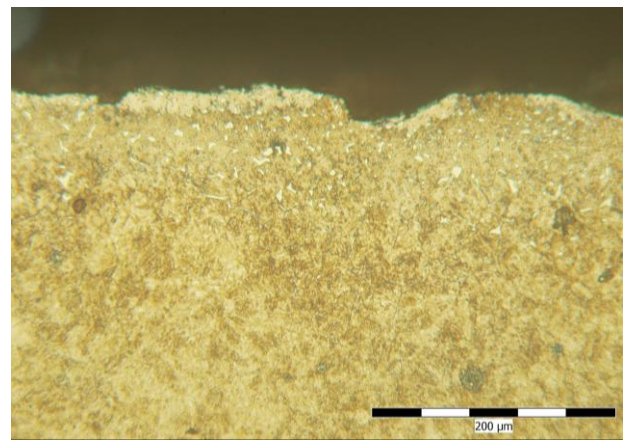
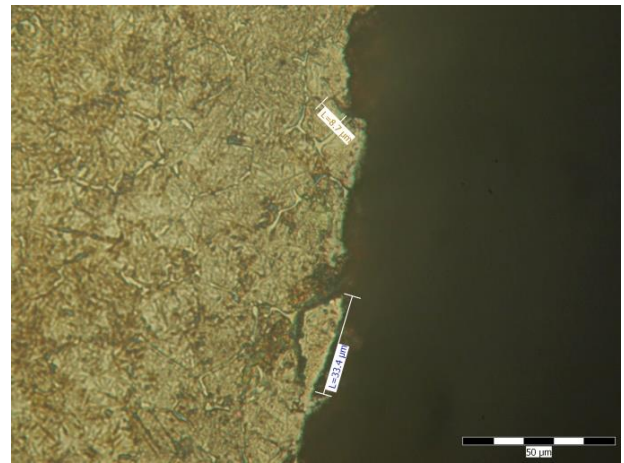


**Figure 14.** Pieces of TP2 specimen

In case of the TP2 specimen several developed cracks have been found, starting

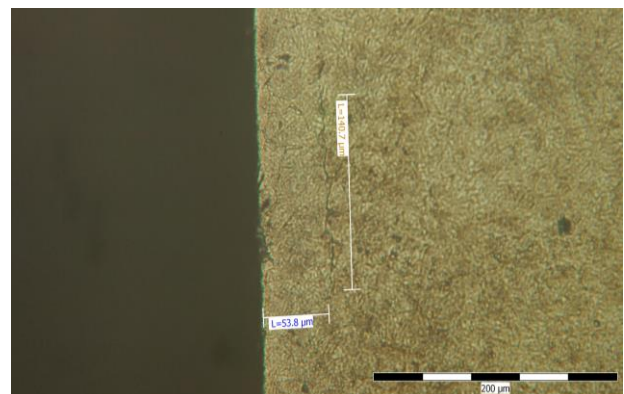
mainly from the edge of the contact zone as it is shown on the Fig. 14, however the test of the TP2 specimen was stopped before any trigger sign from surface damage. It shows that the incubation time was very short, the lifetime was almost 8 times longer, and crack propagation period cannot be neglected.

The other specimens show typical surface pitting damage as it shows the Fig. 16 due to the very brittle surface and high subsurface compression stress.



**Figure 15.** Surface pitting on TP5 specimen

In some case subsurface cracks have been observed as well as it is shown on Fig. 16.



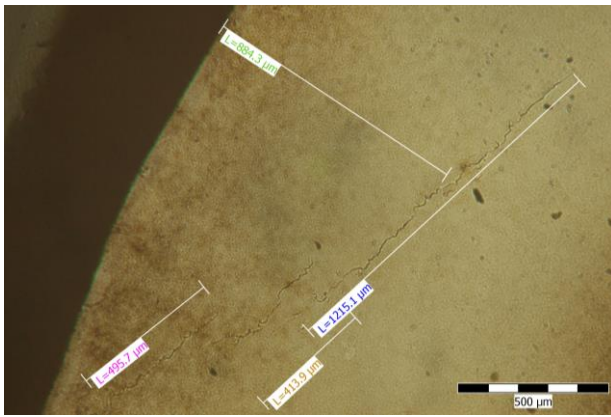


**Figure 16.** Subsurface crack on TP5 specimen

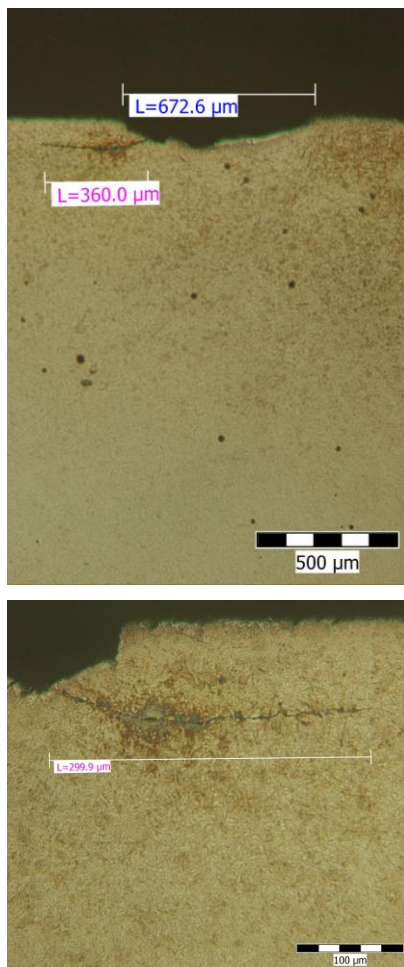


**Figure 17.** Spalling on TP3 specimen

In case of TP3 specimen when the load was the highest spalling damage also can be found.

## 6. CONCLUSION

As a basis for the experimental work, due to the frequent application and previous

experience, the 16MnCr5 case hardening steel was selected. On the sample material made of the model material, the tests were carried out after the workout to validate the numerical model suitable for determining the characteristics of the near-surface layers. Based on a comparison of the results, the model proved to be suitable for determining the layer of the rollers used for contact fatigue testing. Two disc fatigue tests were carried out on five rollers. Microstructural investigations have been started on the rollers. Having proper material characteristics information local approach based modelling will be carried out to study the high cycle fatigue of surfaces under rolling-sliding condition.

## ACKNOWLEDGEMENT

The research was supported by Bilateral Serbian-Hungarian project TÉT\_16-1-2016-0164, the Bolyai Fellowship of the Hungarian Academy of Sciences and the by the únkp-18-4 new national excellence program of the ministry of human capacities. The authors would like to acknowledge the scientific and technical support of Montanuniversität Leoben, Lehrstuhl für Allgemeinen Maschinenbau.

## REFERENCES

- [1] Case-hardening steels, available at: <https://www.schmolz-bickenbach.co.za/>
- [2] G.G. Tibbetts, Diffusivity of carbon in iron and steels at high temperatures, *Journal of Applied Physics*, pp. 4813-4816, 1980.
- [3] P. Maynier et al, Creusot-Loire system for the prediction of the mechanical properties of low alloy steel products. In: Doane D.V. (ed.), Kirkaldy J.S. (ed.): *Hardenability concepts with applications to steel*, Metallurgical Society of AIME, pp. 518-545, 1978.
- [4] W.C. Leslie, *Physical Metallurgy of Steels*, Mc Graw Hill, New York 1982.